A new electronic structure method for doublet states: Configuration interaction in the space of ionized 1*h* and 2*h*1*p* determinants

Anna A. Golubeva, Piotr A. Pieniazek, and Anna I. Krylov[a)]
Department of Chemistry, University of Southern California, Los Angeles, California 90089-0482, USA

(Received 5 December 2008; accepted 18 February 2009; published online 25 March 2009)

An implementation of gradient and energy calculations for configuration interaction variant of equation-of-motion coupled cluster with single and double substitutions for ionization potentials (EOM-IP-CCSD) is reported. The method (termed IP-CISD) treats the ground and excited doublet electronic states of an N-electron system as ionizing excitations from a closed-shell $N+1$-electron reference state. The method is naturally spin adapted, variational, and size intensive. The computational scaling is N^5, in contrast with the N^6 scaling of EOM-IP-CCSD. The performance and capabilities of the new approach are demonstrated by application to the uracil cation and water and benzene dimer cations by benchmarking IP-CISD against more accurate IP-CCSD. The equilibrium geometries, especially relative differences between different ionized states, are well reproduced. The average absolute errors and the standard deviations averaged for all bond lengths in all electronic states (58 values in total) are 0.014 and 0.007 Å, respectively. IP-CISD systematically underestimates intramolecular distances and overestimates intermolecular ones, because of the underlying uncorrelated Hartree–Fock reference wave function. The IP-CISD excitation energies of the cations are of a semiquantitative value only, showing maximum errors of 0.35 eV relative to EOM-IP-CCSD. Trends in properties such as dipole moments, transition dipoles, and charge distributions are well reproduced by IP-CISD. © *2009 American Institute of Physics*. [DOI: 10.1063/1.3098949]

I. INTRODUCTION

Electronic structure calculations of doublet radicals, radical cations, or radical anions, formed when a single bond is broken, as well as upon ionization of or electron attachment to closed-shell species, are challenging due to symmetry breaking and spin contamination of the corresponding open-shell Hartree–Fock (HF) reference.[1,2] Most importantly, symmetry breaking affects not only energies and shapes of potential energy surfaces, but also molecular properties, particularly, charge localization patterns.[3]

Equation-of-motion coupled-cluster methods for ionization potentials and electron attachment (EOM-IP-CC and EOM-EA-CC) offer an elegant solution to this problem by describing target N-electron wave functions as ionized or electron-attached states derived from $(N+1)/(N-1)$ closed-shell references.[4–7] Similar ideas are exploited within symmetry-adapted-cluster configuration-interaction (SAC-CI) framework,[8–10] and even earlier in the CI-based formulation.[11] Both EOM-IP and EOM-EA rely on N-electron closed-shell references and are, therefore, free from the symmetry breaking and spin-contamination problems that are ubiquitous in open-shell calculations. Formal properties of these methods, as well as their numerical performance, e.g., appropriate order of truncation of the CC and EOM expansions, have been studied in great detail.[3–7,12–22] Truncation of both expansions at double excitations offers a reasonable compromise between computational feasibility and accuracy, e.g., the error bars for Koopmans ionization energies (IEs) of closed-shell molecules are about 0.1–0.3 eV, whereas satellite IEs (which correspond to two-electron transitions) may be a couple of eV off.[16] Inclusion of triple and quadrupole excitations reduces the errors for both types of IEs to tenths or even hundredths of eV for both closed- and open-shell references.[16] The computational scaling of the resulting EOM-IP-CCSD method (or simply IP-CCSD) is N^6 due to the CCSD equations for the reference state, whereas the EOM part, the diagonalization of the similarity transformed Hamiltonian $\bar{H}=e^{-T}He^{T}$ in the $1h$ and $2h1p$ space, is N^5.

This work presents a configuration interaction analog of EOM-IP-CCSD. The method termed IP-CISD describes ionized states as $1h$ and $2h1p$ excitations from the closed-shell HF reference and the amplitudes of the target states are found by diagonalizing the bare Hamiltonian H. IP-CISD, which is N^5 approximation to IP-CCSD, is size intensive and variational.

The similarity transformation is crucial for the EOM-CC methods for excitation energies (EOM-EE-CC) because it ensures size intensivity of the excitation energies, which is violated when bare Hamiltonian is diagonalized in the same determinantal space, as done in truncated CI models. However, other EOM methods in which target wave functions and the reference belong to the different sectors of Fock space do not require similarity transformation for size intensivity. For example, the configuration-interaction spin-flip method is rigorously size intensive.[23–26] Likewise, the configuration interaction variant of EOM-IP-CCSD is also size intensive.

[a)]Electronic mail: krylov@usc.edu.

Although the computational cost of SF-CISD is less than that of EOM-SF-CCSD, the computational scaling of both methods is N^6. Of course, SF-CISD is also slightly less accurate[23] than SF-CCSD, as similarity transformation brings in substantial correlation. IP-CISD, however, offers more significant computational savings, as its scaling is only N^5, as opposed to N^6 scaling of EOM-IP-CCSD. Of course, IEs can no longer be accurately described due to the less accurate description of the neutral reference (which is just a HF single-determinant wave function), however, the equilibrium geometries of the target ionized states and their properties (e.g., dipole moments, electronic transition dipole moments, charge distributions), as well as energy differences between the ionized states, can be reproduced reasonably well due to their balanced description within IP-CISD ansatz, as demonstrated by the numerical examples below. Moreover, the IP-CISD wave functions can be used as qualitatively correct zero-order wave functions for a subsequent perturbative treatment. To summarize, IP-CISD is an inexpensive N^5 approximation of the more accurate EOM-IP-CCSD.

The structure of the paper is as follows. Below we describe the IP-CISD method and present programmable energy and gradient expressions, as well as details of implementation within the Q-CHEM electronic structure program.[27] The performance and the capabilities of IP-CISD are demonstrated by calculations of electronic excitation energies and equilibrium geometries of the uracil cation, benzene dimer cations, and ionized water dimer. Ionized noncovalent dimers[3,22,28–31] are excellent test cases due to multiple interacting electronic states and large number of degrees of freedom, which complicates their description by traditional electronic structure methods.

II. THEORY AND IMPLEMENTATION

A. IP-CISD energies

The IP-CISD wave function for state K can be written as

$$\Psi^{\text{IP-CISD}}(K) = (\hat{R}_1(K) + \hat{R}_2(K))\Phi_0, \tag{1}$$

where Φ_0 is the HF determinant of the reference closed-shell system and the second-quantization expressions for the operators $\hat{R}_{1,2}$ are

$$\hat{R}_1(K) = \sum_i r_i(K) i, \tag{2}$$

$$\hat{R}_2(K) = \frac{1}{2}\sum_{ija} r_{ij}^a(K) a^+ ji. \tag{3}$$

In other words, $\hat{R}_1$ and $\hat{R}_2$ generate linear combinations of all possible ionized (i.e., $1h$) and ionized-excited ($2h1p$) determinants with appropriate spin projection (either $M_s=1/2$ or $M_s=-(1/2)$) from the reference:

$$\hat{R}_1(K)\Phi_0 = \sum_i r_i(K)\Phi_i, \tag{4}$$

$$\hat{R}_2(K)\Phi_0 = \frac{1}{2}\sum_{ija} r_{ij}^a(K)\Phi_{ij}^a. \tag{5}$$

The choice of the reference Φ_0 defines the HF vacuum, i.e., the separation of the orbital space into occupied and virtual subspaces, and the ionizing operators $\hat{R}$ are excitation operators with respect to this vacuum. We adhere to the following convention: indices $i,j,\cdots$ are reserved for the orbitals occupied in the reference determinant Φ_0, indices $a,b,\cdots$ to unoccupied orbitals, and $p,q,\cdots$ are used in the general case, i.e., when an orbital can be either occupied or virtual.[31]

The equations for the amplitudes are derived by applying variational principle to the familiar CI energy functional

$$E_K = \frac{\langle \Psi^{\text{IP-CISD}}(K)|H|\Psi^{\text{IP-CISD}}(K)\rangle}{\langle \Psi^{\text{IP-CISD}}(K)|\Psi^{\text{IP-CISD}}(K)\rangle} \tag{6}$$

and are

$$(H - E_0)R = R\Omega, \tag{7}$$

where H is the matrix of the Hamiltonian in the basis of the $1h$ and $2h1p$ determinants, matrix R contains the amplitudes, Ω is a matrix composed of the energy differences with respect to the reference state, $\omega_k = E_K - E_0$, and $E_0 = \langle\Phi_0|H|\Phi_0\rangle$. Thus, the amplitudes and target states energies are found by diagonalization of the Hamiltonian in the $\{\Phi_i, \Phi_{ij}^a\}$ space

$$\begin{pmatrix} H_{SS} - E_0 & H_{SD} \\ H_{DS} & H_{DD} - E_0 \end{pmatrix}\begin{pmatrix} R_1(K) \\ R_2(K) \end{pmatrix} = \omega_K \begin{pmatrix} R_1(K) \\ R_2(K) \end{pmatrix}, \tag{8}$$

where H_{SS}, H_{DS}, and H_{DD} denote $1h-1h$, $2h1p-1h$, and $2h1p-2h1p$ blocks of the Hamiltonian matrix, respectively. These equations are usually solved using the Davidson iterative diagonalization procedure,[32] which requires the computation of the σ-vectors, the products of the Hamiltonian and trial vectors. Programmable expressions for the IP-CISD σ-vectors are

$$\sigma_i = ([H_{SS} - E_0]R_1)_i + (H_{SD}R_2)_i, \tag{9}$$

$$([H_{SS} - E_0]R_1)_i = -\sum_j r_j f_{ij}, \tag{10}$$

$$(H_{SD}R_2)_i = \sum_{jb} r_{ij}^b f_{jb} + \frac{1}{2}\sum_{jkb} r_{jk}^b \langle kj||ib\rangle, \tag{11}$$

$$\sigma_{ij}^a = (H_{DS}R_1)_{ij}^a + ([H_{DD} - E_0]R_2)_{ij}^a, \tag{12}$$

$$(H_{DS}R_1)_{ij}^a = -\sum_k r_k \langle ij||ka\rangle, \tag{13}$$

$$([H_{DD} - E_0]R_2)_{ij}^a = P(ij)\sum_k r_{jk}^a f_{ik} + \sum_b r_{ij}^b f_{ab} - P(ij)\sum_{kb} r_{ik}^b \langle jb||ka\rangle + \sum_{kl} r_{kl}^a \langle ij||kl\rangle. \tag{14}$$

Note that for the closed-shell references, the resulting set of determinants is spin complete, which means that the IP-CISD wave functions are naturally spin adapted. Another

TABLE I. Programmable expressions for the unrelaxed IP-CISD density matrices.

$$\gamma'_{ij}=\tilde{\gamma}_{ij}+\delta_{ij}$$
$$\tilde{\gamma}_{ij}=-\frac{1}{2}P_{+}(ij)\left[r_i r_j+\sum\nolimits_{ka} r^a_{ik} r^a_{jk}\right]$$
$$\gamma'_{ab}=\frac{1}{4}P_{+}(ab)\sum\nolimits_{ij} r^a_{ij} r^b_{ij}$$
$$\gamma'_{ia}=-\sum\nolimits_{j} r_j r^a_{ij}$$

$$\Gamma'_{ijkl}=\tilde{\Gamma}_{ijkl}-\delta_{li}\delta_{kj}+\delta_{ki}\delta_{lj}-\delta_{li}\tilde{\gamma}_{jk}+\delta_{ki}\tilde{\gamma}_{jl}+\delta_{lj}\tilde{\gamma}_{ik}-\delta_{kj}\tilde{\gamma}_{il}$$
$$\tilde{\Gamma}_{ijkl}=\sum\nolimits_{a} r^a_{ij} r^a_{kl}$$
$$\Gamma'_{abcd}=0$$
$$\Gamma'_{ijka}=\tilde{\Gamma}_{ijka}-\delta_{kj}\gamma_{ia}+\delta_{ki}\gamma_{ja}$$
$$\tilde{\Gamma}_{ijka}=-r^a_{ij} r_k$$
$$\Gamma'_{iajb}=\tilde{\Gamma}_{iajb}+\delta_{ji}\gamma_{ab}$$
$$\tilde{\Gamma}_{iajb}=-\sum\nolimits_{k} r^b_{ik} r^a_{jk}$$
$$\Gamma'_{iabc}=0$$
$$\Gamma'_{ijab}=0$$

advantage of this approach stems from its multistate character: multiple ionized states are treated on the same footing and can be computed simultaneously, and their interactions can be properly descried by virtue of Eq. (7). Moreover, since all the states are derived from the common reference, the calculation of transition properties (e.g., transition dipole moments and nonadiabatic and spin-orbital couplings) is not complicated by nonorthogonal orbitals, which is often the case in state-specific multireference approaches involving orbital optimizations.

The gradient calculation of approximate wave functions is complicated by the presence of non-Hellmann–Feynman terms, which account for the presence of constrains on the wave function parameters. These terms can be handled by using Z-vector[33] or Lagrangian[34–39] techniques. The IP-CISD Lagrangian is

$$\mathcal{L}(R,C,\Lambda,\Omega)=\frac{\langle\Phi_0 R|H|R\Phi_0\rangle}{\langle\Phi_0 R|R\Phi_0\rangle}+\frac{1}{2}\sum_{pq}\lambda_{pq}(f_{pq}-\delta_{pq})+\sum_{pq}\omega_{pq}(S_{pq}-\delta_{pq}), \quad (15)$$

where S and C are the overlap and MO matrices, respectively. The C matrix is implicit in the integrals. The two constrains are: (i) the orbitals are eigenfunctions of the Fock operator and (ii) the orbitals are orthonormal. When the constraints are satisfied, the values and derivatives of the Lagrangian and the energy are the same. The only difference between Eq. (17) and Eq. (24) from Ref. 39 (EOM-CCSD Lagrangian) is the presence of the amplitude response terms in the latter. Thus, the equations from Refs. 22 and 39 can be reused by simply excluding the amplitude response terms. The unrelaxed IP-CISD density matrices accounting only for the explicit dependence of the Hamiltonian on the perturbation [the first term in Eq. (15)] are given in Table I. The calculation of the orbital response terms is identical to that described in Refs. 22 and 39. In Eqs. (54) and (55) of Ref. 39, the amplitude response part is simply omitted. Moreover, since the Hamiltonian is not similarity transformed, the density matrices need not be symmetrized.

The IP-CISD energies, analytic gradients and properties calculations are implemented in the Q-CHEM electronic structure package.[27]

III. COMPUTATIONAL DETAILS

Equilibrium geometries of the five lowest ionized states of uracil were optimized using analytic gradients under C_s constraint at the IP-CCSD and IP-CISD levels with the 6-31+G(d) basis set.[40] The cation excitation energies and transition properties were computed at the neutral uracil geometry (optimized by RI-MP2/cc-pVTZ, see Ref. 30) and at the optimized geometry of the lowest electronic state of the cation using the 6-31+G(d) and 6-311+G(d,p) bases,[40,41] with the core electrons frozen.

Permanent dipole moments were computed at the respective optimized geometries using fully relaxed IP-CCSD and IP-CISD one-particle density matrices. Since the dipole moments of charged systems are not origin invariant, all the dipoles were computed relative to the center of mass of the cations.

In water dimer calculations, the geometries of the neutrals from Ref. 29 were employed. The cation geometries were optimized by IP-CISD and IP-CCSD with the 6-311(+,+)G(d,p), 6-311(2+,+)G(d,p), 6-311(2+,+)G(2df), and aug-cc-pVTZ basis sets[40–42] with symmetry constraint.

Benzene dimer calculations were carried out with IP-CISD and IP-CCSD with 6-31(+)G(d) basis and under symmetry constraint, as in Ref. 3. The wave functions for the t-shaped were analyzed using the natural bond orbitals (NBO) (Ref. 43) procedure and the charge of the individual fragments was calculated.

All optimizations were conducted using default Q-CHEM optimization thresholds: the gradient and energy tolerance were set to 3×10^{-4} and 1.2×10^{-3}, respectively; maximum energy change was set to 1×10^{-6}. The IP-CCSD geometries of the benzene dimer isomers were computed using tighter thresholds.[22] All electrons were correlated in the uracil, water dimer, and benzene dimer geometry optimizations and properties calculations.

Figures 1 and 2 provide the definitions of the geometric parameters for uracil, water dimer, and three benzene dimer isomers. All optimized geometries, as well as other relevant information, are provided in supplementary materials.[44]

IV. NUMERICAL RESULTS

A. Equilibrium geometries and electronically excited states of the uracil cation

Uracil has eight different bonds between heavy atoms, as depicted in Fig. 1. Figure 3 shows the values of the CC(1), CO(1), CO(2), and CN(2) bond lengths for the five lowest electronic states of the cation, as well as the corresponding values in the neutrals. The molecular orbitals (MOs) hosting the unpaired electron are also shown. In agreement with molecular orbital considerations, ionization results in significant changes in some bond lengths, which vary from state to

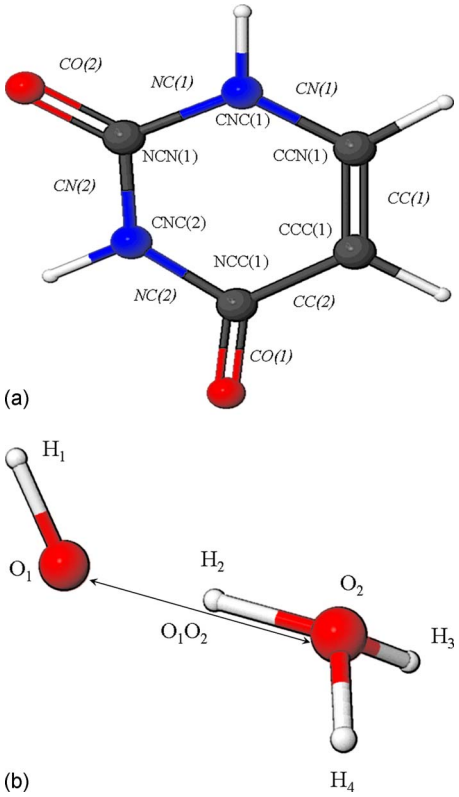

FIG. 1. (Color online) Definitions of the geometric parameters for uracil (upper panel) and water dimer (lower panel) at the proton-transferred geometry.

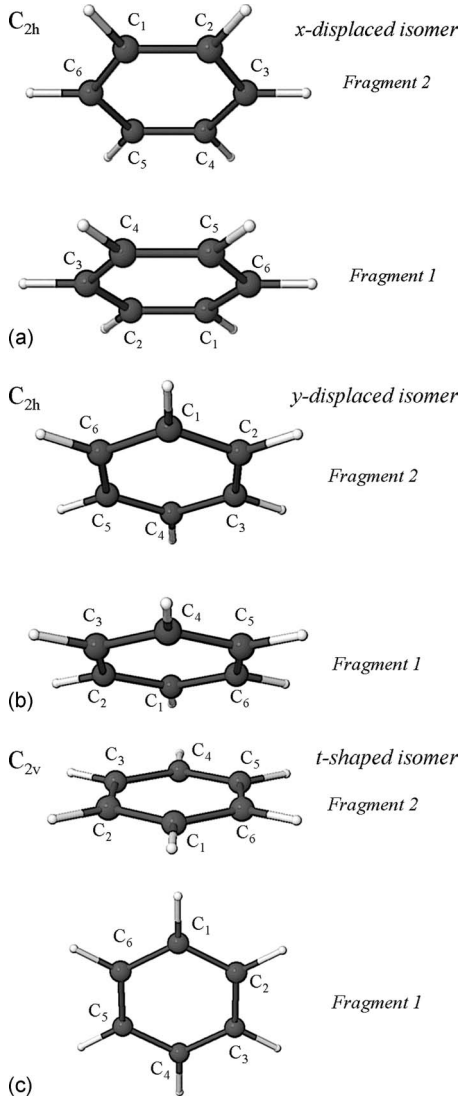

FIG. 2. Definitions of the geometric parameters for three isomers of the benzene dimer: *x*-displaced (top), *y*-displaced (middle), and t-shaped (bottom).

state. For example, the CC(1) bond becomes much longer in the first ionized state derived by ionization from the π_{CC} orbital, whereas the CO bonds undergo significant changes in the states derived by ionization from the respective oxygen lone pairs. As one can see from Fig. 3, IP-CISD systematically underestimates the bond lengths, probably because of the uncorrelated HF reference. However, it reproduces the trends, such as structural differences between the states, very well.

The absolute errors of IP-CISD versus IP-CCSD are summarized in Table II. For the bond lengths, the IP-CISD errors are always negative. The table also presents average absolute errors and standard deviations for each state, which are around 0.014–0.016 and 0.007–0.010 Å, respectively. Absolute average error and standard deviation for these eight bonds in five electronic states are 0.015 and 0.008 Å, respectively.

The results for six bond angles are summarized in Table III. Figure 4 visualizes changes in CNC(2) angle upon ionization. The results are similar to the bond lengths behavior—IP-CISD reproduces the trend in structural changes very well. Averages absolute error and standard deviation for all angles in the five states are 0.343° and 0.266°, respectively.

The computed permanent dipole moments in the center of mass frame are given in Table IV. The IP-CCSD and IP-CISD values are very similar indicating that IP-CISD reproduces well both the equilibrium structures and electron distributions. IP-CISD values are systematically 0.1–0.2 a.u. too large. Thus, IP-CISD wave functions inherit limitations of the uncorrelated HF reference and are too ionic, as compared to more correlated IP-CCSD.

Table V presents vertical excitation energies and transition dipole moments of the uracil cation at two different geometries, i.e., the geometry of the neutral and the equilibrium geometry of the lowest ionized state. IP-CISD errors are 0.1–0.3 eV and they are consistently larger for the low-lying states. Overall, the order of states is reproduced correctly, however, IP-CISD excitation energies are of semiquantitative accuracy only.

Intensities of transitions are in qualitative agreement. Most importantly, both methods agree which states are dark and which are bright, indicating that the underlying wave functions are qualitatively similar. Other important trends, e.g., the lowering of the transition dipoles for the two highest states upon geometric relaxation (from the neutral to the cation), are also reproduced. The basis set dependence of the errors is small, as evidenced by the results in two different bases.

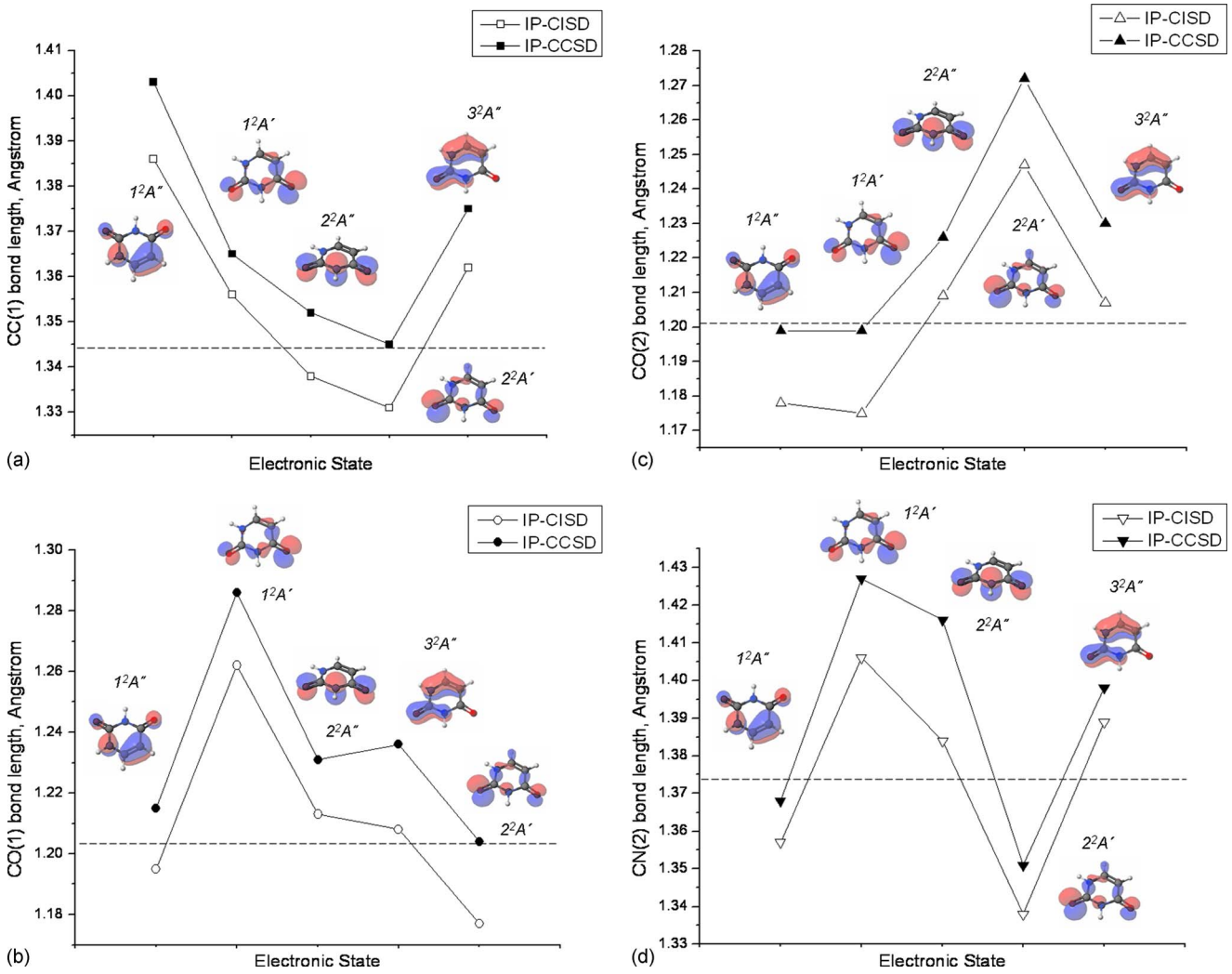

FIG. 3. (Color online) Selected bond lengths in the five lowest electronic states of the uracil cation. The corresponding values of the neutral are shown by dashed lines. The MOs from which electron is removed are shown for each state.

B. Equilibrium geometries of the three isomers of the benzene dimer cation

Geometrical parameters (see Fig. 2) for the three isomers of the benzene dimer cation are summarized in Table VI and visualized in Fig. 5. From this example, we investigate how well IP-CISD reproduces the structures of the ionized noncovalent dimers. Ionization of such systems changes the bonding from noncovalent to covalent, which results in significant structural changes, in particular the interfragment distance. For example, the interfragment distance shrinks from 3.9 to 3.3 Å in the sandwich isomers. IP-CISD overestimates the interplanar separation in the displaced sandwich

TABLE II. The IP-CCSD bond lengths (Å) in the five electronic states of the uracil cation and absolute errors (in parenthesis) of IP-CISD relative to IP-CCSD.

Bonds	$1\,^2A''$	$1\,^2A'$	$2\,^2A''$	$2\,^2A'$	$3\,^2A''$
CC(1)	1.403(0.017)	1.365(0.009)	1.352(0.014)	1.345(0.014)	1.375(0.013)
CN(1)	1.321(0.005)	1.357(0.013)	1.390(0.012)	1.392(0.010)	1.471(0.028)
NC(1)	1.460(0.027)	1.386(0.009)	1.358(0.011)	1.351(0.010)	1.371(0.017)
CN(2)	1.386(0.011)	1.427(0.021)	1.416(0.032)	1.351(0.013)	1.398(0.009)
NC(2)	1.403(0.016)	1.341(0.003)	1.426(0.029)	1.387(0.007)	1.425(0.009)
CC(2)	1.469(0.012)	1.423(0.010)	1.444(0.001)	1.459(0.003)	1.473(0.005)
CO(1)	1.215(0.020)	1.286(0.024)	1.231(0.018)	1.236(0.028)	1.204(0.027)
CO(2)	1.199(0.021)	1.199(0.024)	1.226(0.017)	1.272(0.025)	1.230(0.023)
Average abs. error	0.016	0.014	0.017	0.014	0.016
Standard deviation	0.007	0.008	0.010	0.009	0.009

TABLE III. The IP-CCSD angles (deg) in the five electronic states of the uracil cation and absolute errors (in parentheses) of IP-CISD relative to IP-CCSD.

Bonds	$1\,^2A''$	$1\,^2A'$	$2\,^2A''$	$2\,^2A'$	$3\,^2A''$
CCN(1)	119.217(0.156)	122.529(0.078)	122.648(0.280)	121.826(0.223)	120.745(0.728)
CNC(1)	125.636(0.152)	124.334(0.232)	123.333(0.621)	121.309(0.101)	122.446(0.027)
NCN(1)	113.077(0.496)	112.381(0.584)	113.977(1.260)	118.079(0.225)	114.018(0.215)
CNC(2)	126.733(0.533)	124.291(0.383)	126.224(0.556)	124.315(0.099)	129.409(0.318)
NCC(2)	115.214(0.463)	120.781(0.046)	114.481(0.644)	116.352(0.105)	113.365(0.222)
CCC(1)	120.123(0.429)	115.684(0.093)	119.337(0.447)	118.120(0.145)	120.016(0.430)
Average abs. error	0.372	0.236	0.635	0.150	0.323
Standard deviation	0.172	0.212	0.334	0.060	0.239

isomers, by ca. 0.2 Å, while the sliding displacement is reproduced quite accurately. Similarly, the separation between the rings in the t-shaped structure is overestimated.

In the t-shaped structure the two fragments are nonequivalent and the charge is unevenly distributed between the rings. The degree of charge distribution determines the intensity of charge resonance bands, which can be used to probe the structure and dynamics of the system. The NBO analysis of the IP-CISD densities for the states involved in this transition yields an 0.888 and 0.101 partial charge on fragment 1 (stem), which is in excellent agreement with the IP-CCSD values[3] of 0.880 and 0.099, respectively. Charge-resonance transition energies are 0.71 and 0.81 eV for EOM-IP-CCSD and IP-CISD, respectively.

The changes in intramolecular parameters are reproduced by IP-CISD very well; average absolute error in bond lengths is for all three isomer is 0.01 Å. Note that Jahn–Teller displacements in the t-shaped isomer are also accurately described. The contraction of the interfragment distance is reproduced correctly, however, the distance is overestimated. We interpret this by the absence of dispersion in uncorrelated HF reference employed by IP-CISD. The absolute error is slightly larger owing to the larger distance.

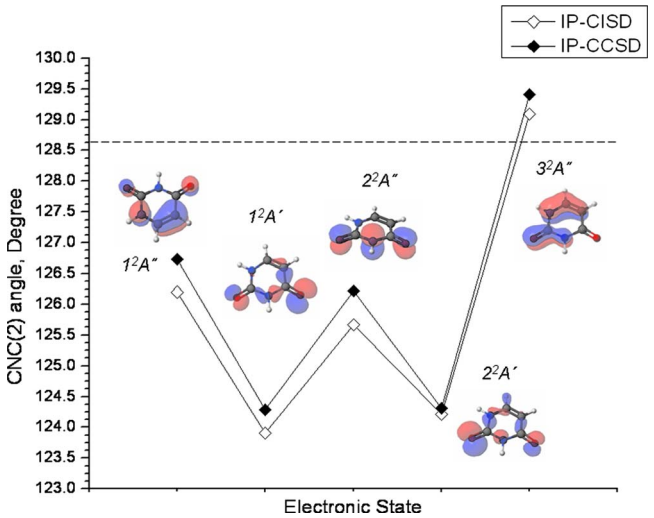

FIG. 4. (Color online) The CNC(2) angle in the five lowest electronic states of uracil cation. Dashed line shows the corresponding value at the geometry of neutral.

C. Water dimer cation

Table VII summarizes geometrical parameters (see Fig. 1) for the two lowest electronic states of the water dimer cation. Selected bond lengths and angles are visualized in Fig. 6. The errors for the intramolecular parameters are similar to those in uracil and benzene dimers.

The trends in intramolecular distances are similar to the benzene dimer cations, however, in this case ionization introduces even stronger perturbation to electronic structure and leads to the proton transfer and formation of $OH\cdots H_3O^+$ complex, as evident from the value of O_1H_2 distance in Table VII. The OO bond length shortens by about 0.3 Å in the lowest ionized state relative to the neutral. The values of the OO distance between the two lowest ionized states differ by about 0.06 Å. IP-CISD reproduces these trends and structural differences between the different ionized states correctly.

The absolute errors for the intermolecular parameters are slightly larger, e.g., 0.05–0.06 Å for the OO distance, however, one should keep in mind that the value of this bond is about 2.5 Å. As in the benzene dimer example, IP-CISD overestimates the intramolecular distances.

An important result is that the errors of IP-CISD relative to IP-CCSD are not very sensitive to the basis set, as one might expect in view of different amounts of correlation included in the latter. The absolute average errors in bond lengths for electronic states are 0.043, 0.044, 0.037, and 0.040 Å in the 6-311(+,+)G(d,p), 6-311(2+,+)G(d,p), 6-311(2+,+)G(2df), and aug-cc-pVTZ bases, respectively.

D. Timings

To demonstrate gains in computational cost, we present timings for IP-CCSD and IP-CISD calculations of the uracil dimer on a Xeon 3.2 GHz Linux machine using parallel version (threaded over two processors) of the CCSD and EOM code (the HF and integral transformation modules were not

TABLE IV. IP-CCSD and IP-CISD permanent dipole moments (a.u.) of the five lowest electronic states of the uracil cation computed at the respective optimized geometries relative to the center of mass.

	$1\,^2A''$	$1\,^2A'$	$2\,^2A''$	$2\,^2A'$	$3\,^2A''$
IP-CCSD	2.509	1.474	1.144	1.384	2.641
IP-CISD	2.632	1.602	1.279	1.511	2.759

TABLE V. The IP-CCSD and IP-CISD excitation energies (eV) and transition dipole moments (a.u.) of the uracil cation at the equilibrium geometries of the neutral and the cation.

	Neutral				Cation			
	IP-CCSD		IP-CISD		IP-CCSD		IP-CISD	
6-31(+)G**	E	μ^2	E	μ^2	E	μ^2	E	μ^2
$1\ ^2A'$	0.668	3.20×10^{-4}	0.367	2.48×10^{-4}	1.175	3.00×10^{-4}	0.820	2.21×10^{-4}
$2\ ^2A''$	1.063	1.2×10^{-6}	0.867	5×10^{-8}	1.809	1.24×10^{-5}	1.577	1.80×10^{-5}
$2\ ^2A'$	1.647	0.790	1.427	0.819	2.385	0.611	2.156	0.613
$3\ ^2A''$	3.566	1.342	3.627	0.955	4.209	0.940	4.223	0.611
Average abs. error		0.195				0.208		
	Neutral				Cation			
	IP-CCSD		IP-CISD		IP-CCSD		IP-CISD	
6-311(+)G**	E	μ^2	E	μ^2	E	μ^2	E	μ^2
$1\ ^2A'$	0.642	2.59×10^{-4}	0.335	1.85×10^{-5}	1.144	2.31×10^{-4}	0.785	1.51×10^{-4}
$2\ ^2A''$	1.037	3.1×10^{-6}	0.848	2.6×10^{-7}	1.779	6.3×10^{-6}	1.557	9.5×10^{-6}
$2\ ^2A'$	1.614	0.786	1.388	0.820	2.349	0.603	2.112	0.611
$3\ ^2A''$	3.543	1.358	3.613	0.968	4.187	0.952	4.209	0.620
Average abs. error		0.198				0.211		

parallelized). The symmetry of the dimer is C_2 and two lowest states in each irrep were requested. In 6-31+G(d) basis (320 basis functions), the wall time for total (including SCF and integral transformation) IP-CCSD and IP-CISD calculations was 5.82 and 1.50 h, respectively. The IP-CISD calculation in 6-311+G(2d,p) basis (480 basis functions) took only 10.5 h.

V. CONCLUSIONS

We reported an implementation of gradient and energy calculation for configuration interaction variant of EOM-IP-CCSD, IP-CISD. The method is naturally spin adapted, variational, and size intensive. The computational scaling is N^5, in contrast with the N^6 scaling of EOM-IP-CCSD, which results in significant computational savings. The performance of the method was benchmarked on the uracil cation (five ionized states), water dimer cation (two electronic states), and three isomers of the benzene dimer cations (ground electronic state). The results demonstrate that the equilibrium geometries of the ionized states are reproduced reasonably well. Using symmetry unique parameters from

TABLE VI. The bond lengths (Å), angles (deg), the interfragment distance and sliding displacements (Å) in the ground state of the *x*-displaced, *y*-displaced, and t-shaped benzene dimer cations calculated with IP-CISD/6-31(+)G(d). For the *x*- and *y*-displaced structures, geometric parameters for only one of the benzene fragments are provided (the fragments are equivalent by symmetry). Absolute errors of IP-CISD relative to IP-CCSD are presented in parentheses. Average absolute errors are calculated using the data for symmetry unique parameters.

Parameter (number)	*x*-displaced	*y*-displaced	t-shaped (fragment 1)	t-shaped (fragment 2)
CH bond range	1.075(0.013)–1.076(0.014)	1.074(0.014)–1.076(0.013)	1.073(0.009)–1.077(0.012)	1.075(0.014)
C_1C_2	1.373(0.010)	1.385(0.011)	1.419(0.010)	1.393(0.012)
C_2C_3	1.408(0.011)	1.414(0.011)	1.376(0.001)	1.387(0.012)
C_3C_4	1.400(0.011)	1.384(0.011)	1.414(0.011)	1.393(0.012)
C_4C_5	1.379(0.010)	1.384(0.011)	1.414(0.011)	1.393(0.012)
C_5C_6	1.400(0.011)	1.414(0.011)	1.376(0.001)	1.387(0.012)
C_6C_1	1.408(0.011)	1.385(0.011)	1.419(0.010)	1.393(0.012)
Average abs. error	0.011	0.011	0.007	0.012
$C_1C_2C_3$	119.569(0.032)	120.473(0.009)	119.428(0.018)	119.933(0.009)
$C_2C_3C_4$	120.807(0.026)	120.307(0.010)	119.282(0.096)	119.933(0.009)
$C_3C_4C_5$	119.607(0.012)	119.301(0.041)	121.514(0.120)	120.133(0.015)
$C_4C_5C_6$	119.607(0.012)	120.307(0.010)	119.282(0.096)	119.933(0.009)
$C_5C_6C_1$	120.807(0.026)	120.472(0.010)	119.428(0.018)	119.933(0.009)
$C_6C_1C_2$	119.569(0.032)	119.092(0.051)	121.065(0.108)	120.133(0.015)
Average abs. error	0.023	0.020	0.078	0.011
Interfr. separation	3.31/3.08	3.31/3.07	4.81/4.58	
Sliding coordinate	1.04/1.07	1.03/1.10	···	

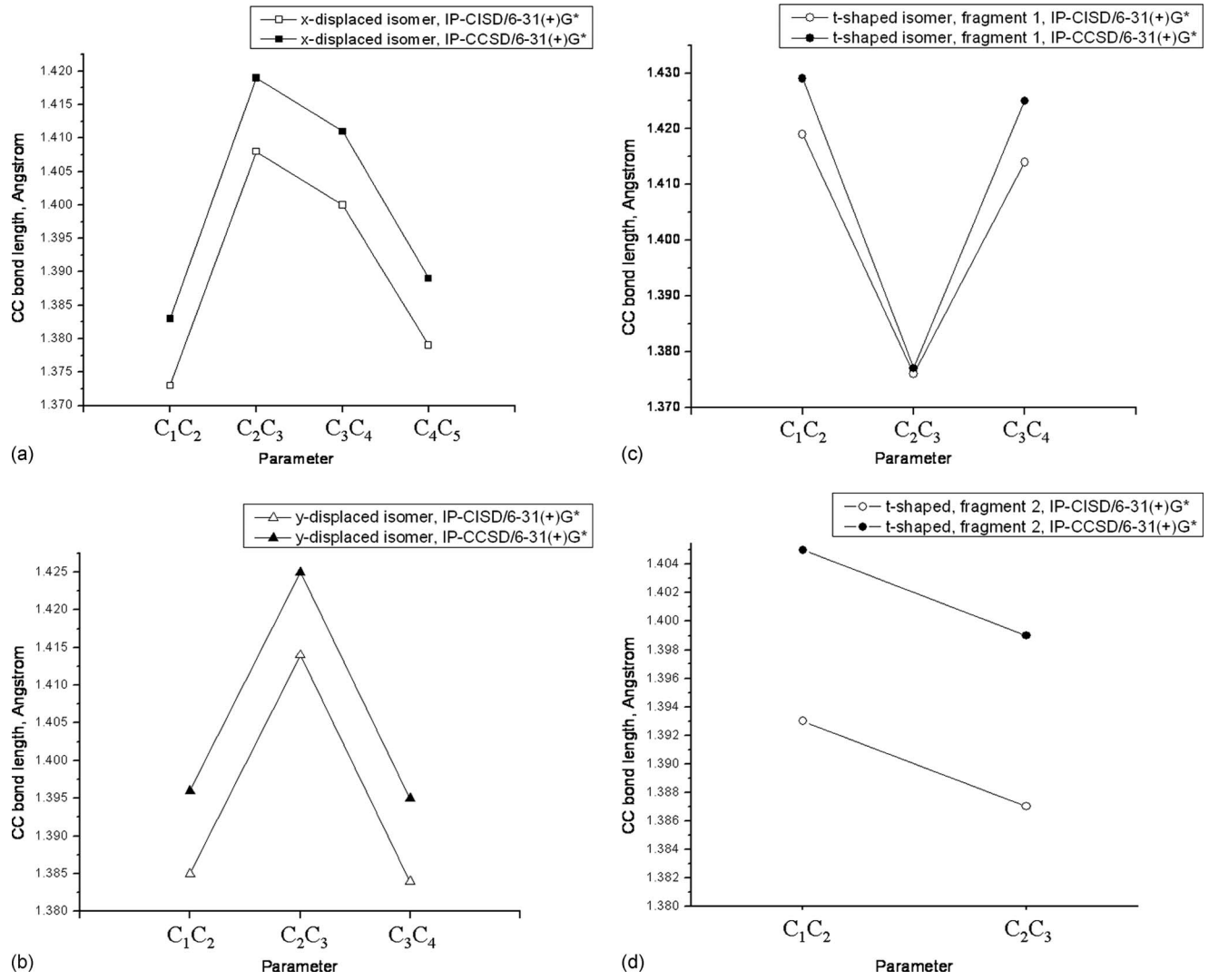

FIG. 5. The CC bond lengths of the three benzene dimer cation isomers in the ground electronic state optimized with IP-CISD/6-31(+)G(d) and IP-CCSD/6-31(+)G(d). Only the values of the symmetry unique parameters for corresponding symmetry nonequivalent fragments are shown.

these ten structures optimized in a modest basis set, we computed average absolute error and standard deviation for bond lengths and angles relative to the IP-CCSD values. For bond lengths, average absolute error and standard deviation are 0.014 and 0.007 Å, respectively, and for angles 0.255° and 0.264°. It is informative to compare these numbers with mean absolute errors and standard deviations of the HF and CCSD methods for well-behaved closed-shell molecules

TABLE VII. The IP-CCSD bond lengths (Å) and angles (deg) in the two electronic states of the water dimer cation and absolute errors (in parentheses) of IP-CISD relative to IP-CCSD calculated with different bases.

	6-311(+,+)G(d,p)		6-311(2+,+)G(d,p)		6-311(2+,+)G(2df)		aug-cc-pVTZ	
Parameter	$1\,^2A''$	$1\,^2A'$	$1\,^2A''$	$1\,^2A'$	$1\,^2A''$	$1\,^2A'$	$1\,^2A''$	$1\,^2A'$
H_1O_1	0.978(0.012)	0.973(0.010)	0.978(0.012)	0.973(0.010)	0.977(0.012)	0.973(0.010)	0.975(0.010)	0.970(0.008)
O_1H_2	1.425(0.127)	1.525(0.081)	1.423(0.128)	1.522(0.083)	1.526(0.082)	1.592(0.083)	1.429(0.115)	1.519(0.079)
H_3O_2	0.970(0.014)	0.971(0.015)	0.970(0.014)	0.971(0.015)	0.972(0.016)	0.973(0.015)	0.968(0.013)	0.970(0.014)
O_2H_4	0.970(0.014)	0.971(0.015)	0.970(0.014)	0.971(0.015)	0.972(0.016)	0.973(0.015)	0.968(0.013)	0.970(0.014)
O_1O_2	2.475(0.082)	2.532(0.060)	2.474(0.082)	2.529(0.062)	2.549(0.054)	2.592(0.062)	2.478(0.074)	2.524(0.061)
$H_1O_1H_2$	123.713(6.795)	176.809(0.522)	123.485(6.881)	176.520(0.671)	126.141 (2.966)	176.858 (0.671)	120.553(6.235)	177.434(0.169)
$H_3O_2H_4$	109.874(2.495)	111.259(2.279)	109.816(2.517)	111.187(2.287)	110.256 (1.302)	111.250 (2.287)	109.902(2.161)	111.147(1.976)
				Average abs. errors				
Bonds	0.050	0.036	0.050	0.037	0.036	0.037	0.045	0.035
Angles	4.645	1.400	4.699	1.479	2.134	1.479	4.198	1.073

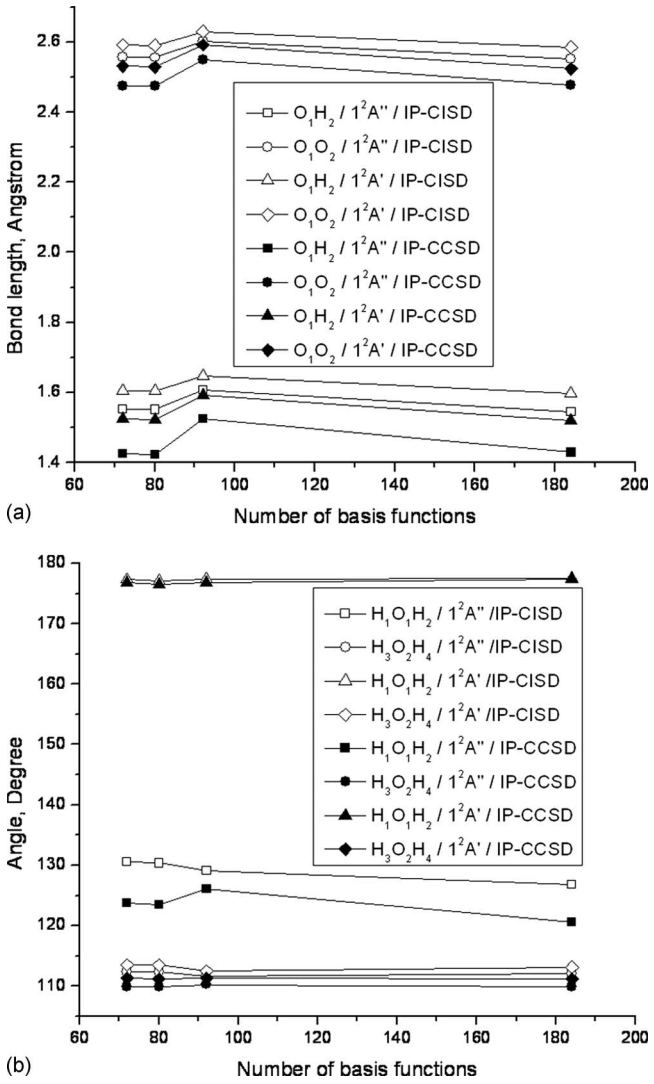

FIG. 6. Selected bond lengths and angles in the two lowest electronic states of the water dimer cation optimized with EOM-IP-CISD and EOM-IP-CCSD with different bases.

relative to the experiment.[34] For bond lengths, the CCSD/cc-pVTZ and CCSD/cc-pVDZ values are 0.0064/0.0066 Å and 0.0119/0.0076 Å, respectively.[34] The HF errors and standard deviations in cc-pVTZ and cc-pVDZ are 0.0263/0.0223 and 0.0194/0.0225, respectively.[34] Thus, IP-CISD structures are of similar quality as HF geometries of closed-shell molecules. Inheriting limitations of the underlying HF reference, IP-CISD systematically underestimates bond lengths and overestimates interfragment distances. Most importantly, IP-CISD correctly reproduces structural changes induced by ionization and structural differences between different ionized states.

Molecular properties such as permanent and transition dipole moments and charge distributions are reproduced very well demonstrating that IP-CISD wave functions are qualitatively correct. IEs cannot be computed by IP-CISD because of the use of uncorrelated HF description of the neutral, however, energy differences between the ionized states are of semiquantitative accuracy (errors of about 0.3 eV relative to IP-CCSD).

Our results suggest that IP-CISD is most useful as an economical alternative for geometry optimization in the ionized systems. Using IP-CISD structures, more accurate energy differences can be computed using more expensive IP-CCSD. Moreover, IP-CISD wave functions may be employed as zero-order wave functions in subsequent perturbative treatment.

ACKNOWLEDGMENTS

This work was conducted in the framework of the *iOpenShell* Center for Computational Studies of Electronic Structure and Spectroscopy of Open-Shell and Electronically Excited Species (iopenshell.usc.edu) supported by the National Science Foundation through the CRIF:CRF Grant Nos. CHE-0625419, 0624602, 0625237, and is also supported by Grant No. CHE-0616271. A.I.K. is grateful to the Institute of Mathematics and its Applications in Minnesota for its hospitality and productive environment during her stay at IMA as a visiting professor.

[1] E. R. Davidson and W. T. Borden, J. Phys. Chem. **87**, 4783 (1983).
[2] N. J. Russ, T. D. Crawford, and G. S. Tschumper, J. Chem. Phys. **120**, 7298 (2004).
[3] P. A. Pieniazek, S. A. Arnstein, S. E. Bradforth, A. I. Krylov, and C. D. Sherrill, J. Chem. Phys. **127**, 164110 (2007).
[4] D. Sinha, D. Mukhopadhyay, and D. Mukherjee, Chem. Phys. Lett. **129**, 369 (1986).
[5] S. Pal, M. Rittby, R. J. Bartlett, D. Sinha, and D. Mukherjee, Chem. Phys. Lett. **137**, 273 (1987).
[6] J. F. Stanton and J. Gauss, J. Chem. Phys. **101**, 8938 (1994).
[7] M. Nooijen and R. J. Bartlett, J. Chem. Phys. **102**, 3629 (1995).
[8] H. Nakatsuji and K. Hirao, J. Chem. Phys. **68**, 2053 (1978).
[9] H. Nakatsuji, K. Ohta, and K. Hirao, J. Chem. Phys. **75**, 2952 (1981).
[10] H. Nakatsuji, Chem. Phys. Lett. **177**, 331 (1991).
[11] J. Simons and W. D. Smith, J. Chem. Phys. **58**, 4899 (1973).
[12] D. Sinha, D. Mukhopadhya, R. Chaudhuri, and D. Mukherjee, Chem. Phys. Lett. **154**, 544 (1989).
[13] J. F. Stanton and J. Gauss, J. Chem. Phys. **111**, 8785 (1999).
[14] Y.J. Bomble, J.C. Saeh, J.F. Stanton, P.G. Szalay, M. Kállay, and J. Gauss, J. Chem. Phys. **122**, 154107 (2005).
[15] S. Hirata, M. Nooijen, and R. J. Bartlett, Chem. Phys. Lett. **328**, 459 (2000).
[16] M. Kamiya and S. Hirata, J. Chem. Phys. **125**, 074111 (2006).
[17] Y. Ohtsuka, P. Piecuch, J. R. Gour, M. Ehara, and H. Nakatsuji, J. Chem. Phys. **126**, 164111 (2007).
[18] M. Musial, S. A. Kucharski, and R. J. Bartlett, J. Chem. Phys. **118**, 1128 (2003).
[19] M. Musial and R. J. Bartlett, J. Chem. Phys. **119**, 1901 (2003).
[20] M. Haque and D. Mukherjee, J. Chem. Phys. **80**, 5058 (1984).
[21] L. Meissner and R. J. Bartlett, J. Chem. Phys. **94**, 6670 (1991).
[22] P. A. Pieniazek, S. E. Bradforth, and A. I. Krylov, J. Chem. Phys. **129**, 074104 (2008).
[23] A. I. Krylov, Chem. Phys. Lett. **350**, 522 (2001).
[24] J. S. Sears, C. D. Sherrill, and A. I. Krylov, J. Chem. Phys. **118**, 9084 (2003).
[25] D. Casanova and M. Head-Gordon, J. Chem. Phys. **129**, 064104 (2008).
[26] D. Casanova, L. V. Slipchenko, A. I. Krylov, and M. Head-Gordon, J. Chem. Phys. **130**, 044103 (2009).
[27] Y. Shao, L. F. Molnar, Y. Jung, J. Kussmann, C. Ochsenfeld, S. Brown, A. T. B. Gilbert, L. V. Slipchenko, S. V. Levchenko, D. P. O'Neil, R. A. Distasio, Jr., R. C. Lochan, T. Wang, G. J. O. Beran, N. A. Besley, J. M. Herbert, C. Y. Lin, T. Van Voorhis, S. H. Chien, A. Sodt, R. P. Steele, V. A. Rassolov, P. Maslen, P. P. Korambath, R. D. Adamson, B. Austin, J. Baker, E. F. C. Bird, H. Daschel, R. J. Doerksen, A. Drew, B. D. Dunietz, A. D. Dutoi, T. R. Furlani, S. R. Gwaltney, A. Heyden, S. Hirata, C.-P. Hsu, G. S. Kedziora, R. Z. Khalliulin, P. Klunziger, A. M. Lee, W. Z. Liang, I. Lotan, N. Nair, B. Peters, E. I. Proynov, P. A. Pieniazek, Y. M. Rhee, J. Ritchie, E. Rosta, C. D. Sherrill, A. C. Simmonett, J. E. Subotnik, H. L. Woodcock III, W. Zhang, A. T. Bell, A. K. Chakraborty, D. M. Chipman, F. J. Keil, A. Warshel, W. J. Herhe, H. F. Schaefer III, J.

Kong, A. I. Krylov, P. M. W. Gill, and M. Head-Gordon, Phys. Chem. Chem. Phys. **8**, 3172 (2006).
[28] P. A. Pieniazek, A. I. Krylov, and S. E. Bradforth, J. Chem. Phys. **127**, 044317 (2007).
[29] P. A. Pieniazek, J. VandeVondele, P. Jungwirth, A. I. Krylov, and S. E. Bradforth, J. Phys. Chem. A **112**, 6159 (2008).
[30] A. A. Golubeva and A. I. Krylov, Phys. Chem. Chem. Phys. **11**, 1303 (2009).
[31] P. A. Pieniazek, E. J. Sundstrom, S. E. Bradforth, and A. I. Krylov, J. Phys. Chem. A (in press) DOI:10.1021/jp811059z.
[32] E. R. Davidson, J. Comput. Phys. **17**, 87 (1975).
[33] N. C. Handy and H. F. Schaefer III, J. Chem. Phys. **81**, 5031 (1984).
[34] T. Helgaker, P. Jørgensen, and J. Olsen, *Molecular electronic structure theory* (Wiley, New York, 2000).
[35] P. G. Szalay, Int. J. Quantum Chem. **55**, 151 (1995).
[36] S. R. Gwaltney and R. J. Bartlett, J. Chem. Phys. **110**, 62 (1999).
[37] F. Furche and R. Ahlrichs, J. Chem. Phys. **117**, 7433 (2002).
[38] P. Celani and H.-J. Werner, J. Chem. Phys. **119**, 5044 (2003).
[39] S. V. Levchenko, T. Wang, and A. I. Krylov, J. Chem. Phys. **122**, 224106 (2005).
[40] W. J. Hehre, R. Ditchfield, and J. A. Pople, J. Chem. Phys. **56**, 2257 (1972).
[41] R. Krishnan, J. S. Binkley, R. Seeger, and J. A. Pople, J. Chem. Phys. **72**, 650 (1980).
[42] T. H. Dunning, J. Chem. Phys. **90**, 1007 (1989).
[43] E. D. Glendening, J. K. Badenhoop, A. E. Reed, J. E. Carpenter, J. A. Bohmann, C. M. Morales, and F. Weinhold, *NBO 5.0., Theoretical Chemistry Institute* (University of Wisconsin, Madison, WI, 2001).
[44] See EPAPS Document No. E-JCPSA6-130-005913 for optimized geometries and relevant information. For more information on EPAPS, see http://www.aip.org/pubservs/epaps.html.